



Deposited via The University of Leeds.

White Rose Research Online URL for this paper:

<https://eprints.whiterose.ac.uk/id/eprint/92791/>

Version: Accepted Version

Article:

Ardestani, MM, Moazen, M and Jin, Z (2014) Gait modification and optimization using neural network-genetic algorithm approach: Application to knee rehabilitation. *Expert Systems with Applications*, 41 (16). pp. 7466-7477. ISSN: 0957-4174

<https://doi.org/10.1016/j.eswa.2014.06.034>

© 2014, Elsevier. Licensed under the Creative Commons Attribution-NonCommercial-NoDerivatives 4.0 International <http://creativecommons.org/licenses/by-nc-nd/4.0/>

Reuse

Items deposited in White Rose Research Online are protected by copyright, with all rights reserved unless indicated otherwise. They may be downloaded and/or printed for private study, or other acts as permitted by national copyright laws. The publisher or other rights holders may allow further reproduction and re-use of the full text version. This is indicated by the licence information on the White Rose Research Online record for the item.

Takedown

If you consider content in White Rose Research Online to be in breach of UK law, please notify us by emailing eprints@whiterose.ac.uk including the URL of the record and the reason for the withdrawal request.

Gait Modification and Optimization using Neural Network-Genetic Algorithm Approach: Application to Knee Rehabilitation

Marzieh.M.Ardestani^{1,*}, Mehran Moazen² and Zhongmin Jin^{1,3}

¹ *State Key Laboratory for Manufacturing System Engineering, School of Mechanical Engineering, Xi'an Jiao tong University, 710054, Xi'an, Shaanxi, China*

² *Medical and Biological Engineering, School of Engineering, University of Hull, Hull, UK*

³ *Institute of Medical and Biological Engineering, School of Mechanical Engineering, University of Leeds, Leeds, LS2 9JT, UK*

*Corresponding author Tel.: +0-86-029-83395122;

E-mail: mostafavizadeh@yahoo.com

Abstract

Gait modification strategies play an important role in the overall success of total knee arthroplasty. There are a number of studies based on multi-body dynamic (MBD) analysis that have minimized knee adduction moment to offload knee joint. Reducing the knee adduction moment, without consideration of the actual contact pressure, has its own limitations. Moreover, MBD-based framework that mainly relies on iterative trial-and-error analysis, is fairly time consuming. This study embedded a time-delay neural network (TDNN) in a genetic algorithm (GA) as a cost effective computational framework to minimize contact pressure. Multi-body dynamic and finite element analyses were performed to calculate gait kinematics/kinetics and the resultant contact pressure for a number of experimental gait trials. A TDNN was trained to learn the nonlinear relation between gait parameters (inputs) and contact pressures (output). The trained network was then served as a real-time cost function in a GA-based global optimization to calculate contact pressure associated with each potential gait pattern. Two optimization problems were solved: first, knee flexion angle was bounded within the normal patterns and second, knee flexion angle was allowed to be increased beyond the normal walking. Designed gait patterns were evaluated through multi-body dynamic and finite element analyses.

The TDNN-GA resulted in realistic gait patterns, compared to literature, which could effectively reduce contact pressure at the medial tibiofemoral knee joint. The first optimized gait pattern reduced the knee contact pressure by up to 21% through modifying the adjacent joint kinematics whilst knee flexion was preserved within normal walking. The second optimized gait pattern achieved a more effective pressure reduction (25%) through a slight increase in the knee flexion at the cost of considerable increase in the ankle joint forces. The proposed approach is a cost-effective computational technique that can be used to design a variety of rehabilitation strategies for different joint replacement with multiple objectives.

Keywords: *Gait modification, Tibiofemoral knee joint, Time delay neural network, Genetic algorithm, Contact pressure*

1 **1. Introduction:**

2 Following total knee arthroplasty (TKA), rehabilitation strategies are of significant importance to accelerate
3 patient recovery (Isaac et al., 2005, Klein et al., 2008), reinforce joint functionality (Moffet et al., 2004, Rahmann et
4 al., 2009), decrease gait asymmetry (Zeni Jr et al., 2011), and augment the durability and life time of knee
5 prostheses (Fransen, 2011, Mont et al., 2006). Gait rehabilitations mainly aim to decrease knee joint loading through
6 minor changes in human gait patterns. However, recognizing the synergistic kinematic changes, required for joint
7 offloading, is a challenging task, hence; computational approaches have been used to facilitate the design procedure.
8 To best of our knowledge, most of the current literature on gait modification strategies have been designed through
9 multi-body dynamic (MBD) analysis (Barrios et al., 2010, Barrios and Davis, 2007, Fregly et al., 2009, Hunt et al.,
10 2008, Mündermann et al., 2008, Willson et al., 2001, Ackermann and van den Bogert, 2010, Anderson and Pandy,
11 2001, Fregly et al., 2007) . However, iterative “trial-and-error” MBD analysis, that has been performed in such
12 studies, is fairly time demanding which limits the applicability and generality of the method. Hence, a cost-effective
13 computational framework that minimizes the computational cost is of particular interest.

14 Besides the computational cost, there are a number of aspects that have not been well addressed by the
15 conventional MBD-based framework. *First* , MBD-based approach attempts to reduce the peak values of knee
16 adduction moment (KAM) which is not always a reliable measure since decreasing KAM may not necessarily
17 decrease knee joint loading (Walter et al., 2010); and the results of such approach are sensitive to the chosen
18 reference frame (e.g. laboratory, floating reference frames) (Lin et al., 2001, Shull et al., 2012). *Second* , joint-
19 offloading gait patterns are likely to decrease the contact area of articulating surfaces that unfavorably may increase
20 the contact pressure at the knee joint (D'Lima et al., 2008). Therefore, reducing the contact pressure should be
21 concerned as the principal goal of rehabilitation design. Conventional computational frameworks however are
22 inherently unable to consider the contact pressure in the design procedure since the conventional methods require an
23 explicit cost function whilst the relation between gait kinematics and the resultant contact pressure has not been
24 stated explicitly before. Also, predicting the contact pressure requires implementing finite element analysis (FEA)
25 which in turn increases the computational cost (Halloran et al., 2010). A cost-effective surrogate which releases the
26 necessity of iterative FEA is therefore of significant advantage. *Third*, previous studies could not reach a general
27 consensus about the contribution of knee flexion to the knee joint offloading. Knee flexion is a key synergetic
28 parameter that is often increased within the clinical execution of the rehabilitation patterns (Barrios et al., 2010,
29 Fregly et al., 2007, van den Noort et al., 2013). Several studies concluded that increasing the knee flexion would
30 reduce KAM (Fregly et al., 2009, Fregly, 2008, Fregly et al., 2007), whilst others showed that it has no association
31 with KAM (Creaby et al., 2013) or may even increase contact pressure at the knee bearing surfaces (D'Lima et al.,

32 2008). A systematic investigation is required to enhance our understanding of the contribution of knee flexion to
33 the knee joint offloading.

34 Artificial neural networks (ANN) and genetic algorithm (GA) are two relatively new techniques in the field
35 of biomechanics. Artificial neural network (ANN) can be used as a real-time surrogate model with the ability to
36 *learn* a nonlinear relationship. Once a set of inputs and corresponding outputs are presented to the network, it will
37 then “learn” the causal interactions between inputs and outputs. Given a new set of inputs, the trained neural network
38 (surrogate model) can generalize the relationship to produce the associated outputs. The ANN surrogate therefore
39 can be of significant advantage especially when the original model necessitates repeating a time-consuming
40 computation. For example, ANN has been widely used as a surrogate of FEA (Campoli et al., 2012, Hambli, 2010,
41 Hambli, 2011, Naito and Torii, 2005, Lu et al., 2013, Simic et al., 2011, Zadpoor et al., 2012). Genetic algorithm is a
42 time-efficient global optimization technique which searches the entire data space to find the best solution (Goldberg,
43 1989). In each iteration, only potential candidates that better optimize the cost function will survive to the next
44 iteration. Thus, regardless of the initial point, the search data space is iteratively modified and GA will rapidly
45 converge to the global optimum solution. This in turn assures the robustness of the method and minimizes the
46 computational effort required to find the best solution. Moreover, GA is capable of dealing with multivariable data
47 space, nonlinear input-output interactions and non-explicit, non-differential cost function.

48 Therefore, the overall aim of this study was to develop a hybrid framework of time delay neural network
49 (TDNN) and genetic algorithm (GA) to address the aforementioned limitations of the literature. In particular this
50 study aimed to (1) optimize the gait pattern in order to minimize the contact pressure at the knee articulating surfaces
51 and (2) investigate the role of knee flexion in knee joint offloading. The advantage of the proposed approach was
52 also compared over the existing knee rehabilitations in the literature.

53 **2. Materials and methods**

54 The proposed computational approach was implemented in the following steps:

55 *Step 1*) Experimental gait analysis data were obtained from the literature (Section 2.1), and imported into MBD
56 analysis to calculate gait kinematics and kinetics (Section 2.2). Knee flexion angle and three dimensional knee joint
57 loadings were predicted by MBD, and then served as boundary condition and loading profiles for the finite element
58 simulation to calculate contact pressure (Section 2.3). Gait trials were then outlined via a number of kinematic
59 features and the corresponding maximum contact pressure values (CPRESS-max) (Section 2.4).

60 *Step 2)* A time-delay neural network (TDNN) was trained to learn the nonlinear relationship between kinematic
61 features as inputs and the corresponding CPRESS-max values as output (Section 2.5).

62 *Step 3)* A genetic algorithm (GA) was implemented to search for the optimum kinematic features (optimization
63 variables) which minimized the CPRESS-max at the knee joint bearing surfaces. In this GA, the trained TDNN was
64 served as a real-time cost function to calculate the objective value (CPRESS-max) (Section 2.6).

65 **2.1. Experimental gait data**

66 Experimental gait analysis data of a single subject with unilateral TKA (female, height 167 cm, mass 78.4
67 kg) was obtained from the literature (<https://simtk.org/home/kneeloads>; accessed on June 2013). The subject walked
68 with a variety of different gait patterns including *normal*, *medial thrust*, *trunk sway*, *walking pole*, *bouncy*, *crouch*,
69 *smooth* and *fore foot strike*. *Medial thrust*, *trunk sway* and *walking pole* were knee rehabilitation strategies, designed
70 to decrease KAM, whilst the remaining gait trials were different walking patterns to cover the span of executable gait
71 for the subject. Compared to *normal* walking, the subject walked with a slightly decreased pelvis obliquity, slightly
72 increased pelvis axial rotation and leg flexion to implement *medial thrust* pattern. For *trunk sway* pattern, the subject
73 walked with an increased lateral leaning of the trunk in the frontal plane over the standing leg. In *walking pole*, the
74 subject used bilateral poles as walking aids. For each gait pattern, five gait trials were repeated under the same
75 walking condition at a self-selected pace. A total of two complete gait cycles were picked up from each trial, leading
76 to a total of 84 data sets. For further details, see (Fregly et al., 2012). Gait trials were recorded in terms of marker
77 trajectory data (Motion Analysis Corp., Santa Rosa, CA) and ground reaction forces (AMTI Corp., Watertown, MA).

78 **2.2. Multi-body dynamic**

79 Experimental ground reaction forces and marker trajectories were imported into the three-dimensional multi-
80 body dynamic simulation software, AnyBody Modelling System (version 5.2, AnyBody Technology, Aalborg,
81 Denmark). A lower extremity musculoskeletal model was used in AnyBody software based on the University of
82 Twente Lower Extremity Model (TLEM) (Klein Horsman, 2007). This model, available in the AnyBody published
83 repository, had 160 muscle units as well as foot, thigh, patella, shank, trunk and thorax segments. Hip joint was
84 modelled as a spherical joint with three degrees of freedom (DOF): flexion-extension, abduction-adduction and
85 internal-external rotation. Knee joint was modelled as a hinge joint with only one DOF for flexion-extension and
86 universal joint was considered for ankle-subtalar complex. Since the assumptions of the simplified knee joint and
87 rigid multi-bodies were made, the detailed knee implant was not considered in the MBD analysis. Knee flexion angle
88 and three dimensional knee joint loads, aligned in medial-lateral, proximal-distal and anterior-posterior directions,
89 were calculated for each complete gait cycle. A complete gait cycle was defined as the time period from heel strike of

90 one leg to the following heel strike of the same leg (Vaughan et al., 1992). Computations were then normalized to
91 100 samples to represent one complete gait cycle. Knee flexion and three dimensional knee joint loads then served as
92 the boundary condition and load profiles for FEA.

93 **2.3. Finite element method**

94 A typical tibiofemoral knee implant was modelled in the commercial finite element package;
95 ABAQUS/Explicit (version 6.12 Simulia Inc., Providence, RI) using the computer aided design (CAD) of a clinically
96 available fixed bearing knee implant. The knee implant consisted of two main parts; femoral component and tibia
97 insert. Rigid body assumptions were applied to both parts, with a simple linear elastic foundation model defined
98 between the two contacting bodies (Halloran et al., 2005). Tetrahedral (C3D10M) elements were used to mesh the
99 model in ABAQUS. Convergence was tested by decreasing the element size from 8 mm to 0.5 mm in five steps (8, 4,
100 2, 1, and 0.5 mm). The solution converged on contact pressure ($\leq 5\%$) with over 86000 and 44000 elements
101 representing the femoral component and the tibia insert respectively. This was also consistent with the previous
102 mesh convergence studies for similar finite element models (Abdelgaied et al., 2011, Halloran et al., 2005). The
103 physical interaction between femoral component and tibia insert was taken into account as a surface-to-surface
104 contact (femur as the master surface and tibia as the slave surface) through a penalty-based approach with an
105 isotropic friction coefficient of 0.04 (Abdelgaied et al., 2011, Halloran et al., 2005). The tibia insert was constrained
106 in all available DOFs and the femoral component was only allowed for flexion-extension under the three dimensional
107 load which were obtained from MBD analysis. The model calculated the contact pressure at each node for each time
108 increment. An output field was created over all simulation frames to compute the maximum value of the contact
109 pressures (CPRESS_max) over the entire gait cycle. Since the medial compartment experiences the CPRESS-max
110 value (Schipplein and Andriacchi, 1991), this part was considered for the rest of the study (Figure 1a).

111 **2.4. Feature extraction**

112 During a complete gait cycle, the extent to which a joint can be moved (range of motion) and the
113 corresponding absolute values of motions directly affect the quality of human gait and joint loading. For example,
114 increasing the “*maximum*” value of hip adduction angle or hip internal rotation would decrease the “*peak*” values of
115 KAM (Barrios et al., 2010). On the other hand, to design a realistic gait modification strategy, the overall trend of
116 kinematic patterns cannot differ significantly from natural human walking habitudes; otherwise the pattern would not
117 be acceptable and executable by the patient. Thus, only the key features of kinematic waveforms are needed to be
118 modified whilst the overall trends should be preserved consistent. Gait kinematics were therefore outlined through a

total of 39 descriptive kinematic features (Table 1 and Figure 1b). These features have been suggested in the literature for a number of studies such as gait analysis (Collins et al., 2009, Gates et al., 2012a, Gates et al., 2012b), gait classification (Armand et al., 2006), evaluation of joint loading (Simonsen et al., 2010), and joint inter-coordination (Wang et al., 2009). Kinematic features (optimization variables) were then allowed to vary within the corresponding ranges of experimental values plus $\pm 20\%$ variations to cover a thorough span of executable movement patterns for the subject. Contact pressure was also characterized by the maximum pressure value occurred over the entire gait cycle (CPRESS-max).

2.5. Time-delay neural network

Time delay neural network (TDNN) was implemented to model the highly nonlinear relationship between kinematic features (39 inputs) and CPRESS-max values (one output). The trained network was then embedded in an optimization process (GA) as a real-time cost function to calculate the objective values (CPRESS-max). The TDNN architecture consisted of a feed forward neural network in which a tapped delay line was added to the input layer (Figure 2). Similar to other types of neural networks, a number of processor units (neurons) were arranged in a certain configuration (layers). A weighted sum of all inputs was fed into each hidden neuron where an activation function acted on this weighted sum to produce the output of the hidden neuron. All of the hidden neurons were activated using “hyperbolic tangent sigmoid” function which linearly scaled its input signal to $[-1, 1]$ interval:

$$y_j^m = \frac{2}{1 + \exp(-2 * V_j^m)} - 1 \quad j = 1, 2, \dots, M_m \quad (1)$$

Where y_j^m is the output of j^{th} hidden neuron located at the m^{th} hidden layer, M_m is the number of hidden neurons at the m^{th} hidden layer, and $V_j^m(n)$ is the weighted sum of the signals from the previous layer which was fed to the j^{th} hidden neuron of m^{th} hidden layer:

$$V_j^m = \sum_{k=1}^{M_{m-1}} (y_k^{m-1} * W_{jk}) + b_j \quad j = 1, 2, \dots, M_m, \quad k = 1, 2, \dots, M_{m-1} \quad (2)$$

Where W_{jk} is the weight relating the output of k^{th} neuron located at the $(m-1)^{th}$ layer (y_k^{m-1}) to the j^{th} hidden neuron at the m^{th} hidden layer with the bias value of b_j , and M_m and M_{m-1} are the number of neurons at the m^{th} and $(m-1)^{th}$ layers respectively. A weighted sum of all hidden neurons' outputs was also fed into the single output node which was activated by a “pure line” function:

$$y_{out} = \sum_{k=1}^{M_m} w_k y_k^m + \bar{y} \quad (3)$$

145 in which \bar{y} is the output bias .

146 TDNN was trained using the scaled conjugate gradient algorithm (SCG) (Møller, 1993). The available data
 147 space, obtained from MBD and FEA, was randomly divided into three main parts: train (70%), validation (15%) and
 148 test (15%) subsets. The train and validation subsets were used to train the network whilst the test subset was not
 149 included in training. The network prediction error on the validation subset implied how accurate the network has
 150 learned the input-output causal relationship (accuracy). On the other hand, the network prediction error on the test
 151 subset indicated the extent to which the trained network could generalize this causal relationship for new inputs
 152 (generality). Generally speaking, the structure of the FFANN would build a trade-off between “*prediction accuracy*”
 153 and “*generality*”. Whilst increasing the number of hidden neurons/layers would increase the prediction accuracy,
 154 using too many neurons would decrease the generality and increase the test error. The number of hidden layers and
 155 hidden neurons were therefore determined according to the network prediction error for the test and validation
 156 subsets. The input delay was also determined by trial and error.

157 2.6. Genetic algorithm

158 In the present study, gait optimization was stated as follows:

$$159 \text{ Minimize } Y : Y=U(X) \quad AX \leq b \quad , \quad X_L \leq X \leq X_U \quad (4)$$

160 Where Y is the CPRESS-max, X is the optimization variables (kinematic features), and U is the trained TDNN. Upper
 161 and lower bounds of the optimization variables (X_L and X_U) were obtained from the experimental gait trials plus \pm
 162 20% variations. Matrix A and vector b described the linear inequality constraints in order to control the natural trends
 163 of the gait kinematics (Appendix). Genetic algorithm (GA) was used to search for those kinematic features that could
 164 minimize CPRESS-max. Kinematic features (optimization variables) were configured as $1*N$ arrays called
 165 individuals ($N=39$). In each iteration, the GA created a population of individuals and then employed the trained
 166 TDNN to calculate the resultant CPRESS-max values associated with potential individuals. Those individuals that
 167 led to lower CPRESS-max values were assigned a higher survivorship probability to be selected and make the next
 168 population. Each individual is indeed a potential solution and each population is a search space of solutions.
 169 Accordingly, after passing several iterations, the population (solution search space) evolved toward the optimized
 170 individuals.

171 The first population was initialized with random individuals in which features of gait kinematics were
 172 randomly chosen due to X_L and X_U . The next populations were created through selected individuals by elitism,

173 crossover and mutation operators of GA (Goldberg, 1989). Table 2 summarizes the setting of the proposed GA in
174 MATLAB (v.2009, Genetic Algorithm toolbox). In the present study, two systematic optimizations were performed:
175 *first*, knee flexion was bounded to vary within the *normal* walking. *Second*, the knee flexion was allowed to vary
176 beyond the *normal* walking up to the *medial thrust* pattern. Once the GA converged to the optimum kinematic
177 features, a typical normal gait cycle was adjusted to these optimum features using the curve fitting technique and the
178 optimized gait pattern was reconstructed. Figure 3 shows schematic of the proposed combined TDNN-GA
179 methodology in this study.

180 3. Results

181 3.1. Network training

182 A four-layer TDNN with four delay units at its input layer , 20 hidden neurons at the first hidden layer and 15
183 hidden neurons at the second one, was trained using 70% of the generated data base. Then, it was validated and tested
184 with the remaining 30%. Figure 4 shows the average performance of the proposed network over 100 training and
185 testing repetitions, each time with a random selection of subsets(Iyer and Rhinehart, 1999). According to the results,
186 the TDNN could accurately predict CPRESS-max values for the training, validation and test subsets. Pearson
187 correlation coefficients, between network predictions (Y axis) and real outputs (X axis), were all above $p=0.98$.
188 Figures 4a, b show that the network learned the nonlinear interaction of kinematics and contact pressure variables
189 ($p=0.99$). Figure 4c shows that the network could predict the CPRESS-max values corresponding to new sets of
190 kinematics which were not included in the training data space ($p=0.98$).

191 3.2. Optimization problem

192 The crossover fraction substantially affects the convergence of GA. Optimization was therefore run for a
193 variety of different values of crossover fraction ranged from 0 to 1 in the step size of 0.05. The crossover fraction of
194 0.85 led to the lowest CPRESS-max value (see Figure 5). Thus, this value was adopted for the rest of this study. In
195 the first optimization problem, knee flexion angle was bounded within *normal* walking. The algorithm was
196 terminated after 75 populations due to stall generation criterion, in which the average change of the objective value
197 (CPRESS-max) was less than 10^{-6} (function tolerance) over 50 populations (stall generations). Figure 6a shows the
198 mean and the best CPRESS-max values associated with each population. After successful convergence of the
199 algorithm, TDNN-GA achieved the lowest CPRESS-max value of 25.58 MPa for the best individual of the last
200 population.

201 Using curve fitting technique, a typical normal gait cycle was adjusted to the obtained optimum kinematic
202 features and the optimized gait pattern was reconstructed (Figure 7). The optimized kinematics laid within the
203 experimental gait patterns suggesting that it would be feasible for the subject to execute the optimized pattern. Using
204 multi-body dynamic analysis, the corresponding joint loadings were computed and compared with the span of
205 experimental values (Figure 8). Results show that lower extremity joints (ankle, knee and hip) underwent realistic
206 loading conditions i.e. within and with similar pattern to the *experimental* gait trials. Particularly, hip joint loading
207 was generally low in the anterior-posterior direction. A general reduction at the anterior-posterior component of knee
208 joint loading and significant reduction at its medial-lateral component around 40%-60% of the gait cycle occurred.
209 Moreover, the medial-lateral component of ankle joint loading was significantly decreased accompanied with a
210 reduction at its anterior-posterior component around 40%-60% of the gait cycle. Figure 9 shows the resultant
211 distribution of the maximum contact pressure at the medial tibiofemoral joint over the entire gait cycle. The
212 maximum contact pressure was reduced by 21.8% compared to the *normal* walking, while previously published gait
213 modifications were fairly ineffective to decrease the contact pressure magnitudes.

214 In the second optimization problem, X_L and X_U were modified and the knee joint flexion was bounded
215 between *normal* and *medial thrust* patterns. The GA achieved the convergence value of 24.61 MPa after 77
216 populations (Figure 6b). Reconstructed gait kinematics and the resultant joint loading patterns are presented in
217 Figures 7 and 8 respectively. Results demonstrate that the second optimized gait pattern also laid within the span of
218 executable gait patterns. The second optimized gait modification led to a significant reduction at the three
219 dimensional hip joint loading (anterior-posterior, proximal-distal and medial-lateral) around 0-25% of the gait cycle.
220 This pattern also led to an overall reduction at anterior-posterior component of the knee joint loading. Anterior-
221 posterior and medial-lateral components of the ankle joint loading were substantially low at 0-25% of the gait cycle,
222 however ankle joint loading was slightly increased around 40%-60% of the gait cycle. By comparison, the second
223 optimization problem yielded to a more effective gait modification pattern that better reduced the magnitude of the
224 contact pressure by up to 25% (Figure 9).

225 4. Discussion

226 4.1. Hybrid neural network-genetic algorithm

227 Neural network was employed: *first*, to model the highly nonlinear relationship between gait kinematics and
228 contact pressure; *second*, to serve as a real-time cost function that allowed the optimization algorithm to be
229 performed in a reasonable computation time. A recent study by Lu et al. (2013) demonstrated that the dynamic

230 structure of a time delay neural network was preferred for modelling the relation between tibiofemoral cartilage load
231 (input) and von Mises stress (output), compared to the traditional static feed forward neural network. Therefore, this
232 structure was used in this study. Moreover, neural network has been used to calculate joint loading from ground
233 reaction forces and gait kinematics (Ardestani et al., 2013, Ardestani et al., 2014) and ground reaction force from gait
234 kinematics (Oh et al., 2013, Ren et al., 2008). In this study, neural network was employed to calculate the contact
235 pressure from gait kinematics. The high correlation that was found between the target values and the network
236 predictions for validation and test subsets reassures the reliability of the proposed structure. The TDNN in turn
237 necessitated involving the GA as the optimization technique. In fact, other classical optimization approaches mainly
238 rely on iterative derivation of an explicit cost function however TDNN modelled the problem non-explicitly.

239 **4. 2. Current research contribution**

240 There are a number of implications on the gait modification and optimization both in terms of methodology and
241 findings. Major limitations of the previous studies were addressed in the present research. *First*, compared to
242 previous studies in which iterative “trial-and-error” MBD analysis has been used, this study presented a cost-
243 effective computational alternative. TDNN provided a real-time cost function for the GA that could rapidly evaluate
244 the contact pressure associated with each potential gait pattern. Moreover, GA is a stochastic direct search method in
245 which the search data space is modified iteratively. This in turn reduced the computational effort required to find the
246 optimized solution. It should be pointed out that although various gait modifications have been developed in
247 association with knee joint offloading, none of them have yet been accepted as a general modification strategy. In
248 fact, due to the large inter-patient variability, reported in gait kinematics and joint loading patterns (Kutzner et al.,
249 2010, Taylor et al., 2004), gait rehabilitation strategies should be determined patient specifically. Hence, to design a
250 gait modification strategy, it is crucial that the proposed computational method is cost-effective and easy to recreate.

251 *Second*, unlike the previous studies in which KAM reduction has been the principal goal of gait modification,
252 here, contact pressure was adopted as a more accurate criterion for knee joint offloading. This in turn built more
253 confidence in the efficiency of the proposed gait modification. Previous gait modifications were mainly designed to
254 reduce knee joint moment. Although these modification patterns could decrease knee joint loading, none of them
255 could decrease contact pressure at the knee joint bearing surfaces whilst the proposed gait pattern in this study could
256 effectively decrease the contact pressure by up to 25% (see Figure 9).

257 *Third*, whilst previous studies have debated on the influence of increasing knee flexion, this study could
258 address the contribution of knee flexion angle to the knee joint offloading in a systematic manner. Two optimizations
259 were performed: first, knee flexion angle was kept within normal patterns to investigate whether it was possible to

260 decrease knee joint loading through adjacent joints effects. Second, knee flexion was allowed for a non-significant
261 increase. Results showed that in the first optimized gait, contact pressure was reduced by up to 21% whilst knee
262 flexion was preserved within normal walking. In the second optimized pattern, a more effective pressure reduction
263 (25%) was achieved with a slight increase in the knee flexion at the cost of considerable increase in the ankle joint
264 forces at 40-60% of the gait cycle. This observation is consistent with previous studies (Fregly et al., 2007) and
265 suggests that perhaps the first optimization pattern in which joint reaction forces were within the experimental range
266 might be more physiologically feasible. Allowing the knee flexion angle to be more increased led to higher ankle
267 joint loading and a gradual reduction in the contact area which in turn increased contact pressure.

268 Overall, hip adduction, ankle flexion, subtalar eversion, pelvis posterior rotation and pelvis medial-lateral
269 rotation were increased during the stance phase for both optimized gait patterns (see Figure 7). However it should be
270 noted that the exact amount of kinematic changes, compared to normal gait, was not reported in this study since
271 specific gait rehabilitation, designed for a particular subject, may not be equally applicable for other patients.
272 Therefore, the quantitative amount of kinematic variations, compared to normal gait, was not focused in this study.

273 4. 3. Limitations

274 There were several limitations in this study: (1) there was a lack of clinical investigation on the estimated
275 kinematics. Nevertheless, from a technical point of view, the predicted kinematic waveforms are expected to be
276 feasible since the TDNN was trained based on executable walking patterns. Once the network learns this dynamic, it
277 uses this dynamic as the acting function to respond to new sets of inputs. Therefore, it is unlikely that it would
278 generate highly aberrant kinematics. Regardless, further investigations are required to test whether the predicted
279 kinematics is feasible to implement for compensatory or unexpected effects on the other joints or the contra-lateral
280 limb; (2) rigid body constraints were applied to both the femoral and tibia components. Halloran et al.(2005) showed
281 that rigid body analysis of the tibiofemoral knee implant can calculate contact pressure in an acceptable consistence
282 with a full deformable model whilst rigid body analysis would be much more time-efficient. Therefore, in order to
283 produce the training data base, required to train the neural network, rigid body constraints were applied. This was
284 consistent with the present multi-body dynamic analysis in which no detailed modelling on the knee implant was
285 included; (3) a typical knee implant was adopted in the present study. Although this implant has been widely used in
286 literature (Clayton et al., 2006, Dalury et al., 2008, Ranawat et al., 2004, Willing and Kim, 2011) , its dimensions
287 were different from the original knee prosthesis by which the subject was implanted. In fact, the subject was
288 implanted with a custom-made sensor-based prosthesis which was specifically produced to measure *in vivo* knee
289 joint loading(Fregly et al., 2012). Accordingly, in this study , a typical commercial knee implant was preferred to test
the

290 efficiency of the proposed knee rehabilitation patterns. Nevertheless, the proposed methodology should be equally
291 applicable to other implant geometries and (4) the knee joint was modelled with only one DOF (flexion-extension).
292 Although six DOFs are possible for the knee joint, the dominant movement of the knee joint takes place in the
293 sagittal plane and knee joint has been mostly simplified as a hinge joint, especially for the knee rehabilitation design
294 purposes (Ackermann and van den Bogert, 2010, Anderson and Pandy, 2001, Fregly et al., 2007).

295 **5. Conclusion**

296 A time-delay neural network was embedded in a genetic algorithm to predict a gait pattern that would
297 minimize the contact pressure at the knee joint bearing surfaces. The proposed algorithm suggested an optimum gait
298 pattern in which hip adduction, ankle flexion, subtalar eversion , pelvis posterior rotation and pelvis medial-lateral
299 rotation were slightly increased during the stance phase. Compared to the available gait rehabilitations, the proposed
300 gait pattern could decrease the knee contact pressure by up to 25%. Compared to the conventional MBD-based
301 framework in gait rehabilitation design, the present methodology facilitated a more practical and reliable design
302 procedure at a lower computational cost :(1) instead of using knee adduction moment, contact pressure was
303 considered as a more accurate criterion which led to a more efficient gait modification, (2) using the time-delay
304 neural network, the proposed computational framework was considerably faster and time-efficient. The
305 computational framework therefore can be easily repeated for any given subject. Moreover, (3) the conflicting effect
306 of the knee flexion was addressed through two systematic optimization frameworks: (i) knee joint may be offloaded
307 without any changes in the knee flexion angle (ii) a slight increase in the knee flexion angle might better reduce
308 contact pressure but at the cost of ankle joint over loading and (iii) large increase in the knee flexion angle reduced
309 the contact area and yielded to an increase in the contact pressure.

310 Various future direction from this study can be considered: (1) on the methodological level, more rigorous
311 tribological metrics (e.g. wear), constraints (e.g. energy expenditure) or gait balance requirements can be included
312 into the computational framework to enhance the predications; (2) on the validation level, further clinical studies are
313 required to validate the finding of such studies; (3) on a wider application level, the proposed methodology in this
314 study has wider implications in design and development of rehabilitation protocols for broader numbers of subjects
315 and other joints such as hip and ankle.

316 **Conflict of interest statement**

317 The authors have no conflict of interests to be declared.

318 **Acknowledgments**

319 This work was supported by “the Fundamental Research Funds for the Central Universities and national
 320 Natural Science Foundation of China [E050702, 51323007]”.The authors gratefully acknowledge " Grand Challenge
 321 Competition to Predict In Vivo Knee Loads" for releasing the experimental data. The authors would like to thank
 322 Shanghai Gaitech Scientific Instruments Co. Ltd for supplementing AnyBody software used in this study.

323 **References**

- 324 ABDELGAIED, A., LIU, F., BROCKETT, C., JENNINGS, L., FISHER, J. & JIN, Z. 2011. Computational
 325 wear prediction of artificial knee joints based on a new wear law and formulation. *Journal of*
 326 *biomechanics*, 44, 1108-1116.
- 327 ACKERMANN, M. & VAN DEN BOGERT, A. J. 2010. Optimality principles for model-based prediction
 328 of human gait. *Journal of biomechanics*, 43, 1055-1060.
- 329 ANDERSON, F. C. & PANDY, M. G. 2001. Dynamic optimization of human walking. *TRANSACTIONS-*
 330 *AMERICAN SOCIETY OF MECHANICAL ENGINEERS JOURNAL OF BIOMECHANICAL*
 331 *ENGINEERING*, 123, 381-390.
- 332 ARDESTANI, M. M., CHEN, Z., WANG, L., LIAN, Q., LIU, Y., HE, J., LI, D. & JIN, Z. 2014. Feed
 333 forward artificial neural network to predict contact force at medial knee joint: Application to gait
 334 modification. *Neurocomputing*, 139, 114-129.
- 335 ARDESTANI, M. M., ZHANG, X., WANG, L., LIAN, Q., LIU, Y., HE, J., LI, D. & JIN, Z. 2013. Human
 336 lower extremity joint moment prediction: A wavelet neural network approach. *Expert Systems with*
 337 *Applications*.
- 338 ARMAND, S., WATELAIN, E., MERCIER, M., LENSEL, G. & LEPOUTRE, F.-X. 2006. Identification
 339 and classification of toe-walkers based on ankle kinematics, using a data-mining method. *Gait &*
 340 *posture*, 23, 240-248.
- 341 BARRIOS, J. A., CROSSLEY, K. M. & DAVIS, I. S. 2010. Gait retraining to reduce the knee adduction
 342 moment through real-time visual feedback of dynamic knee alignment. *Journal of biomechanics*, 43,
 343 2208-2213.
- 344 BARRIOS, J. A. & DAVIS, I. S. A gait modification to reduce the external adduction moment at the knee: a
 345 case study. 31st Annual Meeting of the American Society of Biomechanics, Stanford, CA, paper,
 346 2007.
- 347 CAMPOLI, G., WEINANS, H. & ZADPOOR, A. A. 2012. Computational load estimation of the femur.
 348 *Journal of the Mechanical Behavior of Biomedical Materials*, 10, 108-119.
- 349 CLAYTON, R. A., AMIN, A. K., GASTON, M. S. & BRENKEL, I. J. 2006. Five-year results of the Sigma
 350 total knee arthroplasty. *The Knee*, 13, 359-364.

351 COLLINS, T. D., GHOUSSAYNI, S. N., EWINS, D. J. & KENT, J. A. 2009. A six degrees-of-freedom
352 marker set for gait analysis: repeatability and comparison with a modified Helen Hayes set. *Gait &*
353 *posture*, 30, 173-180.

354 CREABY, M. W., HUNT, M. A., HINMAN, R. S. & BENNELL, K. L. 2013. Sagittal plane joint loading is
355 related to knee flexion in osteoarthritic gait. *Clinical Biomechanics*, 28, 916-920.

356 D'LIMA, D. D., STEKLOV, N., FREGLY, B. J., BANKS, S. A. & COLWELL, C. W. 2008. In vivo contact
357 stresses during activities of daily living after knee arthroplasty. *Journal of Orthopaedic Research*,
358 26, 1549-1555.

359 DALURY, D. F., GONZALES, R. A., ADAMS, M. J., GRUEN, T. A. & TRIER, K. 2008. Midterm results
360 with the PFC Sigma total knee arthroplasty system. *The Journal of Arthroplasty*, 23, 175-181.

361 FRANSEN, M. Rehabilitation after knee replacement surgery for osteoarthritis. *Seminars in Arthritis and*
362 *Rheumatism*, 2011. Elsevier, 93.

363 FREGLY, B. J. 2008. Computational assessment of combinations of gait modifications for knee
364 osteoarthritis rehabilitation. *Biomedical Engineering, IEEE Transactions on*, 55, 2104-2106.

365 FREGLY, B. J., BESIER, T. F., LLOYD, D. G., DELP, S. L., BANKS, S. A., PANDY, M. G. & D'LIMA, D.
366 D. 2012. Grand challenge competition to predict in vivo knee loads. *Journal of Orthopaedic*
367 *Research*, 30, 503-513.

368 FREGLY, B. J., D'LIMA, D. D. & COLWELL, C. W. 2009. Effective gait patterns for offloading the medial
369 compartment of the knee. *Journal of Orthopaedic Research*, 27, 1016-1021.

370 FREGLY, B. J., REINBOLT, J. A., ROONEY, K. L., MITCHELL, K. H. & CHMIELEWSKI, T. L. 2007.
371 Design of patient-specific gait modifications for knee osteoarthritis rehabilitation. *Biomedical*
372 *Engineering, IEEE Transactions on*, 54, 1687-1695.

373 GATES, D. H., DINGWELL, J. B., SCOTT, S. J., SINITSKI, E. H. & WILKEN, J. M. 2012a. Gait
374 characteristics of individuals with transtibial amputations walking on a destabilizing rock surface.
375 *Gait & posture*, 36, 33-39.

376 GATES, D. H., WILKEN, J. M., SCOTT, S. J., SINITSKI, E. H. & DINGWELL, J. B. 2012b. Kinematic
377 strategies for walking across a destabilizing rock surface. *Gait & Posture*, 35, 36-42.

378 GOLDBERG, D. 1989. *Genetic Algorithms in Search, Optimization, and Machine Learning*, Addison-
379 Wesley, Reading, MA, 1989.

380 HALLORAN, J. P., ACKERMANN, M., ERDEMIR, A. & VAN DEN BOGERT, A. J. 2010. Concurrent
381 musculoskeletal dynamics and finite element analysis predicts altered gait patterns to reduce foot
382 tissue loading. *Journal of biomechanics*, 43, 2810-2815.

383 HALLORAN, J. P., PETRELLA, A. J. & RULLKOETTER, P. J. 2005. Explicit finite element modeling of
384 total knee replacement mechanics. *Journal of biomechanics*, 38, 323-331.

385 HAMBLI, R. 2010. Application of neural networks and finite element computation for multiscale
386 simulation of bone remodeling. *Journal of biomechanical engineering*, 132, 114502.

387 HAMBLI, R. 2011. Numerical procedure for multiscale bone adaptation prediction based on neural
388 networks and finite element simulation. *Finite elements in analysis and design*, 47, 835-842.

389 HUNT, M., BIRMINGHAM, T., BRYANT, D., JONES, I., GIFFIN, J., JENKYN, T. & VANDERVOORT,
390 A. 2008. Lateral trunk lean explains variation in dynamic knee joint load in patients with medial
391 compartment knee osteoarthritis. *Osteoarthritis and Cartilage*, 16, 591-599.

392 ISAAC, D., FALODE, T., LIU, P., I'ANSON, H., DILLOW, K. & GILL, P. 2005. Accelerated rehabilitation
393 after total knee replacement. *The knee*, 12, 346-350.

394 IYER, M. S. & RHINEHART, R. R. 1999. A method to determine the required number of neural-network
395 training repetitions. *Neural Networks, IEEE Transactions on*, 10, 427-432.

396 KLEIN, G. R., LEVINE, H. B. & HARTZBAND, M. A. Pain Management and Accelerated Rehabilitation
397 After Total Knee Arthroplasty. *Seminars in Arthroplasty*, 2008. Elsevier, 248-251.

- 398 KLEIN HORSMAN, M. D. 2007. *The Twente lower extremity model: consistent dynamic simulation of*
399 *the human locomotor apparatus*, University of Twente.
- 400 KUTZNER, I., HEINLEIN, B., GRAICHEN, F., BENDER, A., ROHLMANN, A., HALDER, A., BEIER,
401 A. & BERGMANN, G. 2010. Loading of the knee joint during activities of daily living measured
402 in vivo in five subjects. *Journal of biomechanics*, 43, 2164-2173.
- 403 LIN, C.-J., LAI, K.-A., CHOU, Y.-L. & HO, C.-S. 2001. The effect of changing the foot progression angle
404 on the knee adduction moment in normal teenagers. *Gait & Posture*, 14, 85-91.
- 405 LU, Y., PULASANI, P. R., DERAKHSHANI, R. & GUESS, T. M. 2013. Application of neural networks
406 for the prediction of cartilage stress in a musculoskeletal system. *Biomedical Signal Processing and*
407 *Control*, 8, 475-482.
- 408 MILLER, M. F. 1993. A scaled conjugate gradient algorithm for fast supervised learning. *Neural networks*,
409 6, 525-533.
- 410 MANDERMANN, A., ASAY, J. L., MANDERMANN, L. & ANDRIACCHI, T. P. 2008. Implications of
411 increased medio-lateral trunk sway for ambulatory mechanics. *Journal of biomechanics*, 41, 165-
412 170.
- 413 MOFFET, H., COLLET, J.-P., SHAPIRO, S. H., PARADIS, G., MARQUIS, F. & ROY, L. 2004.
414 Effectiveness of intensive rehabilitation on functional ability and quality of life after first total knee
415 arthroplasty: a single-blind randomized controlled trial. *Archives of physical medicine and*
416 *rehabilitation*, 85, 546-556.
- 417 MONT, M. A., BONUTTI, P. M., SEYLER, T. M., PLATE, J. F., DELANOIS, R. E. & KESTER, M. The
418 future of high performance total hip arthroplasty. *Seminars in Arthroplasty*, 2006. Elsevier, 88-92.
- 419 NAITO, K. & TORII, S. 2005. Effects of laterally wedged insoles on knee and subtalar joint moments.
420 *Arch Phys Med Rehabil*, 86.
- 421 OH, S. E., CHOI, A. & MUN, J. H. 2013. Prediction of ground reaction forces during gait based on
422 kinematics and a neural network model. *Journal of biomechanics*, 46, 2372-2380.
- 423 RAHMANN, A. E., BRAUER, S. G. & NITZ, J. C. 2009. A specific inpatient aquatic physiotherapy
424 program improves strength after total hip or knee replacement surgery: a randomized controlled trial.
425 *Archives of physical medicine and rehabilitation*, 90, 745-755.
- 426 RANAWAT, A. S., ROSSI, R., LORETI, I., RASQUINHA, V. J., RODRIGUEZ, J. A. & RANAWAT, C. S.
427 2004. Comparison of the PFC Sigma fixed-bearing and rotating-platform total knee arthroplasty in
428 the same patient: short-term results. *The Journal of arthroplasty*, 19, 35-39.
- 429 REN, L., JONES, R. K. & HOWARD, D. 2008. Whole body inverse dynamics over a complete gait cycle
430 based only on measured kinematics. *Journal of Biomechanics*, 41, 2750-2759.
- 431 SCHIPPLEIN, O. & ANDRIACCHI, T. 1991. Interaction between active and passive knee stabilizers
432 during level walking. *Journal of Orthopaedic Research*, 9, 113-119.
- 433 SHULL, P. B., SHULTZ, R., SILDER, A., DRAGOO, J. L., BESIER, T. F., CUTKOSKY, M. R. & DELP, S.
434 L. 2012. Toe-in gait reduces the first peak knee adduction moment in patients with medial
435 compartment knee osteoarthritis. *Journal of biomechanics*.
- 436 SIMIC, M., HINMAN, R. S., WRIGLEY, T. V., BENNELL, K. L. & HUNT, M. A. 2011. Gait modification
437 strategies for altering medial knee joint load: A systematic review. *Arthritis Care & Research*, 63,
438 405-426.
- 439 SIMONSEN, E. B., MOESBY, L. M., HANSEN, L. D., COMINS, J. & ALKJAER, T. 2010. Redistribution
440 of joint moments during walking in patients with drop-foot. *Clinical Biomechanics*, 25, 949-952.
- 441 TAYLOR, W. R., HELLER, M. O., BERGMANN, G. & DUDA, G. N. 2004. Tibio-femoral loading during
442 human gait and stair climbing. *Journal of Orthopaedic Research*, 22, 625-632.

- 443 VAN DEN NOORT, J. C., SCHAFFERS, I., SNIJDERS, J. & HARLAAR, J. 2013. The effectiveness of
444 voluntary modifications of gait pattern to reduce the knee adduction moment. *Human movement*
445 *science*.
- 446 VAUGHAN, C. L., DAVIS, B. L. & O'CONNOR, J. C. 1992. *Dynamics of human gait*, Human Kinetics
447 Publishers USA.
- 448 WALTER, J. P., D'LIMA, D. D., COLWELL, C. W. & FREGLY, B. J. 2010. Decreased knee adduction
449 moment does not guarantee decreased medial contact force during gait. *Journal of Orthopaedic*
450 *Research*, 28, 1348-1354.
- 451 WANG, T.-M., YEN, H.-C., LU, T.-W., CHEN, H.-L., CHANG, C.-F., LIU, Y.-H. & TSAI, W.-C. 2009.
452 Bilateral knee osteoarthritis does not affect inter-joint coordination in older adults with gait
453 deviations during obstacle-crossing. *Journal of biomechanics*, 42, 2349-2356.
- 454 WILLING, R. & KIM, I. Y. 2011. Design optimization of a total knee replacement for improved constraint
455 and flexion kinematics. *Journal of Biomechanics*, 44, 1014-1020.
- 456 WILLSON, J., TORRY, M. R., DECKER, M. J., KERNOZEK, T. & STEADMAN, J. 2001. Effects of
457 walking poles on lower extremity gait mechanics. *Medicine and science in sports and exercise*, 33,
458 142-147.
- 459 ZADPOOR, A. A., CAMPOLI, G. & WEINANS, H. 2012. Neural network prediction of load from the
460 morphology of trabecular bone. *Applied Mathematical Modelling*.
- 461 ZENI JR, J., MCCLELLAND, J. & SNYDER-MACKLER, L. 2011. 193 A NOVEL REHABILITATION
462 PARADIGM TO IMPROVE MOVEMENT SYMMETRY AND MAXIMIZE LONG-TERM
463 OUTCOMES AFTER TOTAL KNEE ARTHROPLASTY. *Osteoarthritis and Cartilage*, 19, S96-
464 S97.

Table 1 Description of gait kinematic features

Joint	Kinematic feature	Description
Hip	H1	Hip flexion at initial contact
Hip	H2	Maximum hip extension at stance
Hip	H3	Maximum hip flexion at swing phase
Hip	H4	Hip abduction at initial contact
Hip	H5	Maximum hip adduction at midstance phase
Hip	H6	Maximum hip adduction at stance phase
Hip	H7	Hip external rotation at initial contact
Hip	H8	Maximum hip internal rotation at swing phase
Knee	K1	Knee flexion at initial contact
Knee	K2	Maximum knee flexion at stance
Knee	K3	Maximum knee extension at stance
Knee	K4	Maximum knee flexion at swing phase
Ankle	A1	Ankle flexion at initial contact
Ankle	A2	Maximum ankle dorsiflexion at midstance
Ankle	A3	Maximum ankle dorsiflexion at stance
Ankle	A4	Maximum ankle plantar flexion at swing phase
Subtalar	S1	Subtalar inversion at initial contact
Subtalar	S2	Maximum subtalar eversion at stance
Subtalar	S3	Maximum subtalar inversion at stance
Subtalar	S4	Maximum subtalar eversion at swing
Pelvis	PP1	Maximum posterior tilt of pelvis
Pelvis	PP2	Maximum anterior tilt of the pelvis
Pelvis	PP3	Maximum lateral obliquity of the pelvis
Pelvis	PP4	Maximum medial obliquity of the pelvis
Pelvis	PP5	Pelvis vertical position at initial contact
Pelvis	PP6	Maximum pelvis upward position at stance
Pelvis	PP7	Maximum pelvis downward position at stance
Pelvis	PP8	Maximum pelvis upward position at swing
Pelvis	PR1	Pelvis anterior rotation at initial contact
Pelvis	PR2	Maximum pelvis posterior rotation at stance
Pelvis	PR3	Maximum pelvis posterior rotation at swing
Pelvis	PR4	Pelvis medial rotation at initial contact
Pelvis	PR5	Maximum pelvis lateral rotation at stance
Pelvis	PR6	Maximum pelvis medial rotation at stance
Pelvis	PR7	Maximum pelvis lateral rotation at swing
Pelvis	PR8	Pelvis axial rotation at initial contact
Pelvis	PR9	Maximum pelvis axial rotation to the left at stance
Pelvis	PR10	Minimum pelvis axial rotation to the right at stance
Pelvis	PR11	Maximum pelvis axial rotation to the left at swing

Table 2 Genetic algorithm settings in MATLAB

Genetic algorithm parameter	Value
Population size	50
Scaling function	Rank
Selection function	Tournament
Elite count	2
Crossover fraction	0.85
Crossover function	Single point
Mutation function	Adaptive feasible
Maximum number of generations	100

Figure 1

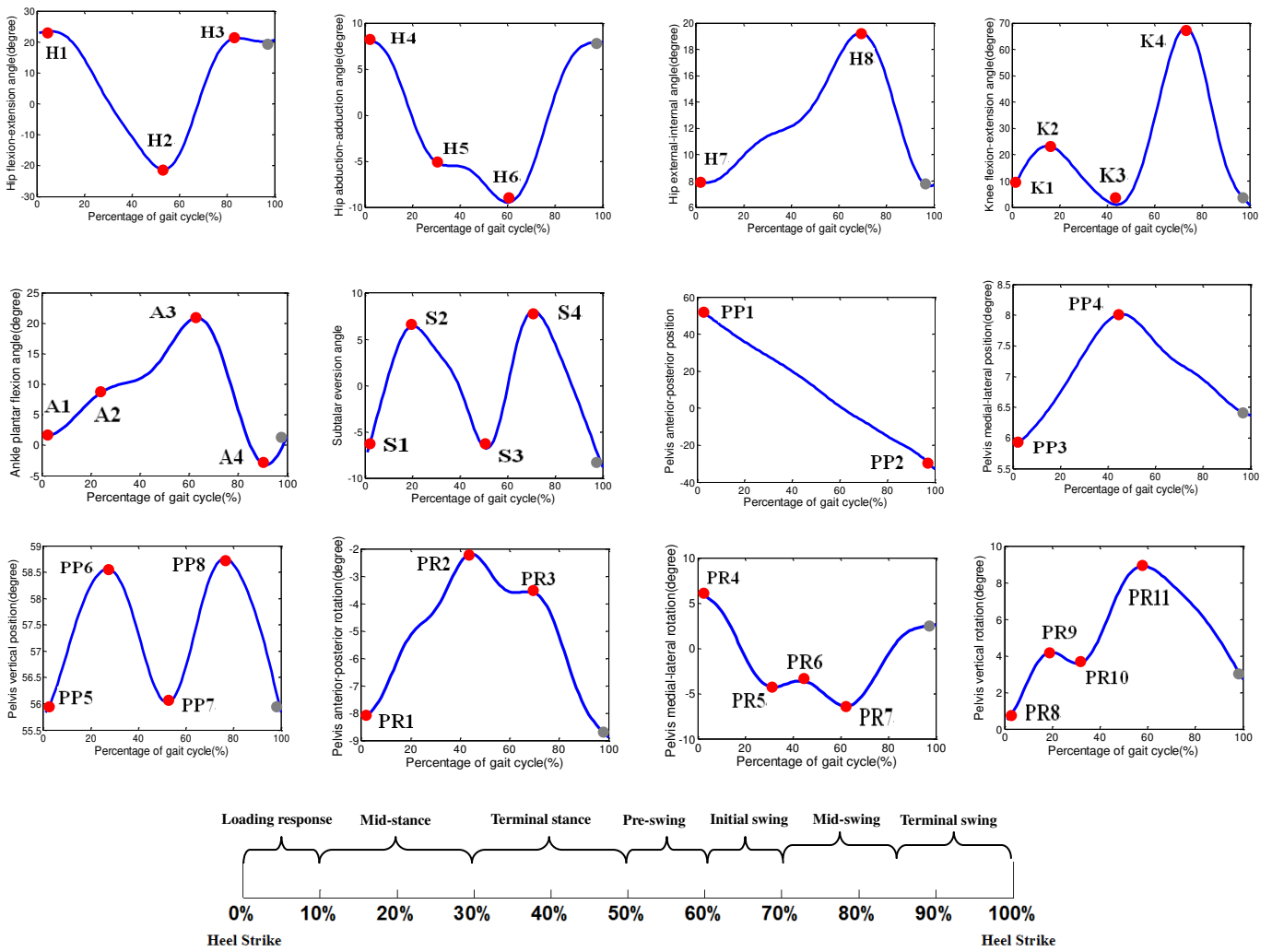
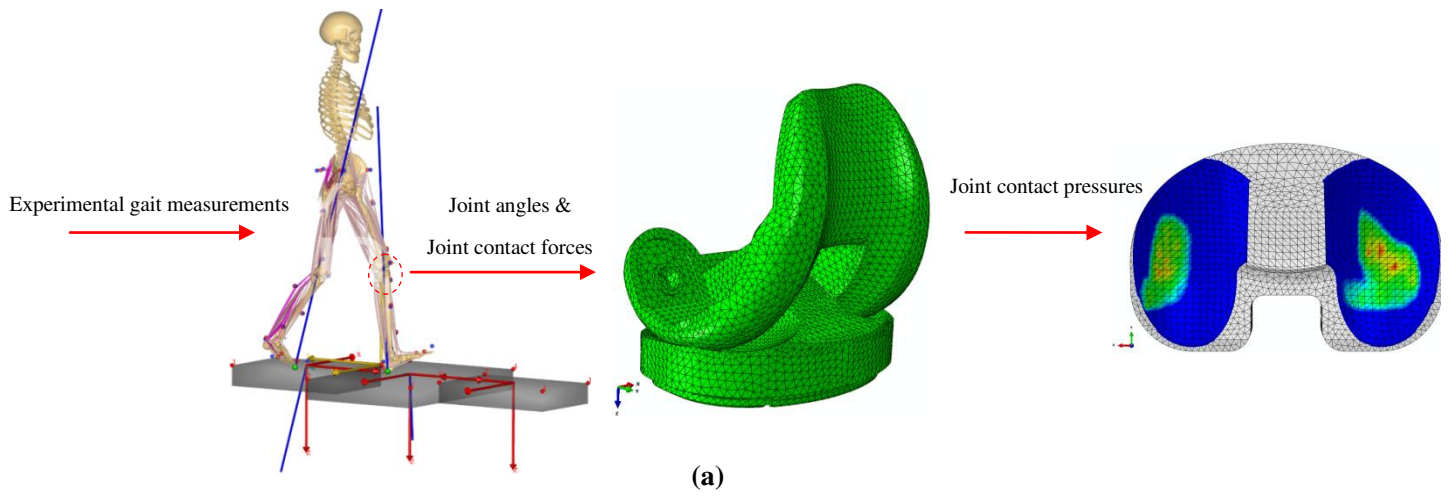


Figure 1 (a) Experimental gait measurements were imported into multi-body dynamics analysis to calculate joint kinematics/kinetics which were then used by finite element analysis to calculate contact pressure (b) Joint angles were parameterized by extremum features (red circles). Due to the periodicity of the gait, joint angle values at the end of the gait cycle (gray points) were equal to the initial values at 0% of the gait cycle except for pelvis anterior-posterior position.

Figure 2

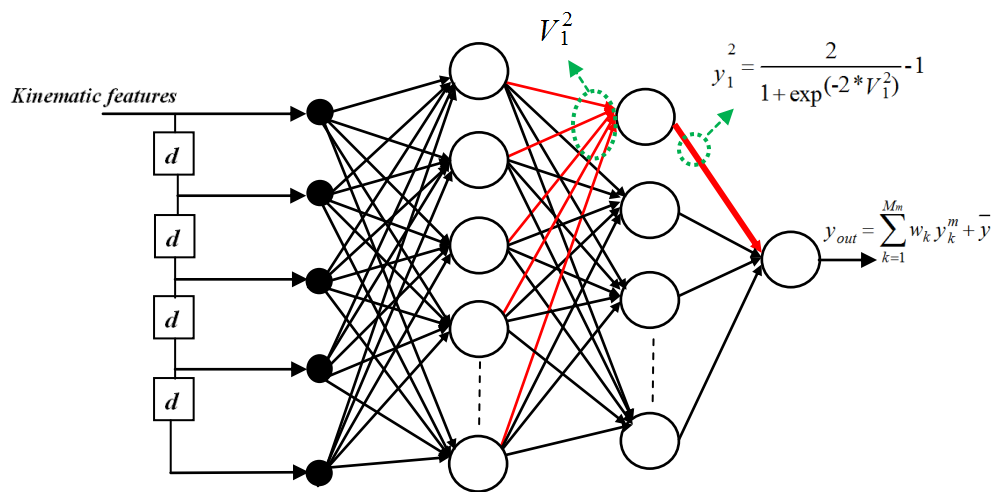


Figure 2 A schematic diagram of a four-layer TDNN used in this study. The network calculated the maximum values of contact pressure (output) based on gait features (inputs).

Figure 3

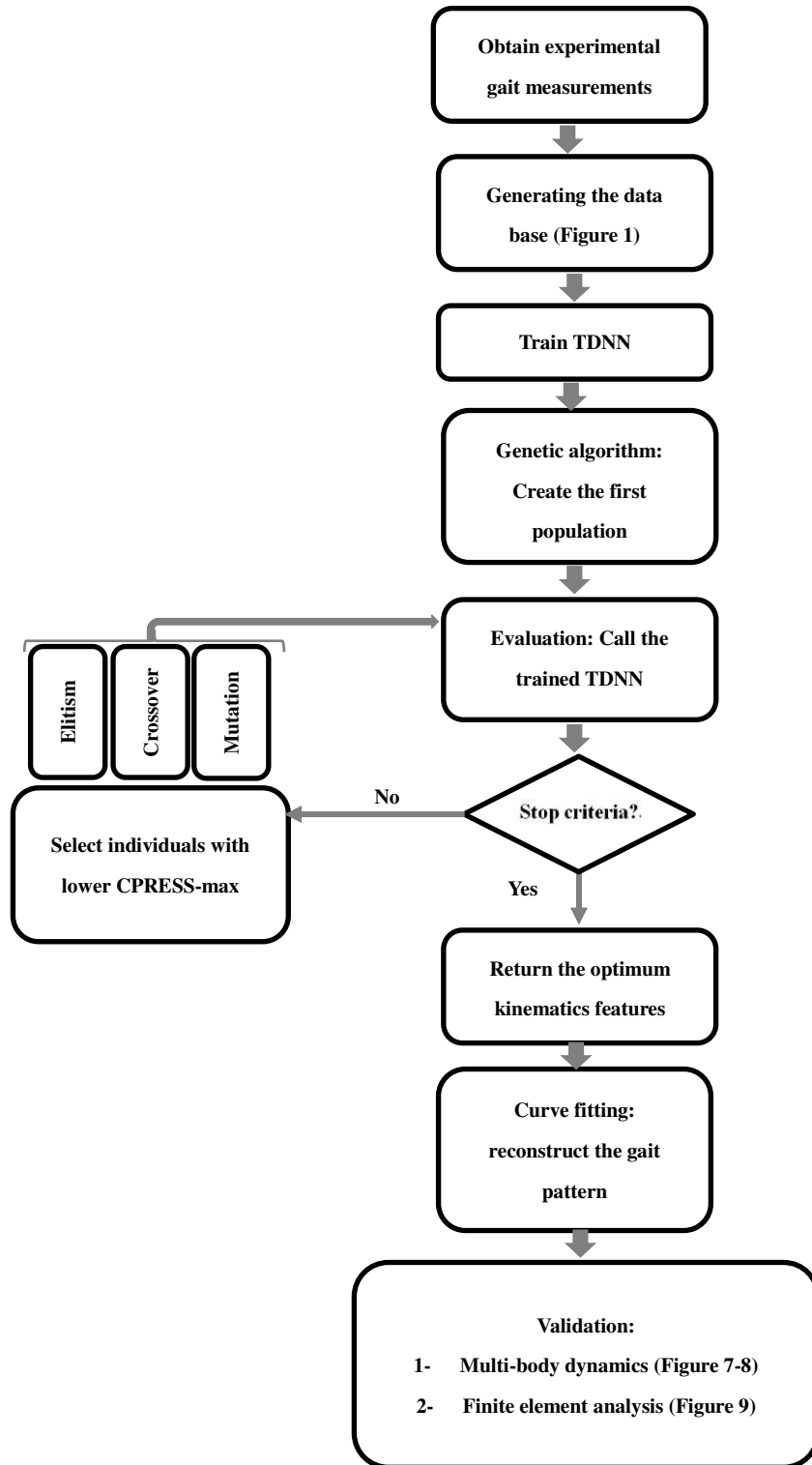


Figure 3 The flowchart of the proposed TDNN-GA.

Figure 4

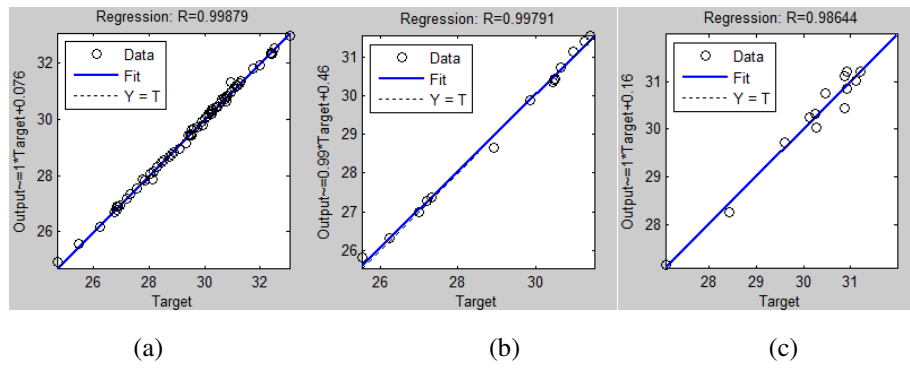


Figure 4 Network predictions versus actual CPRESS-max values for (a) train (b) validation and (c) test subsets.

Figure 5

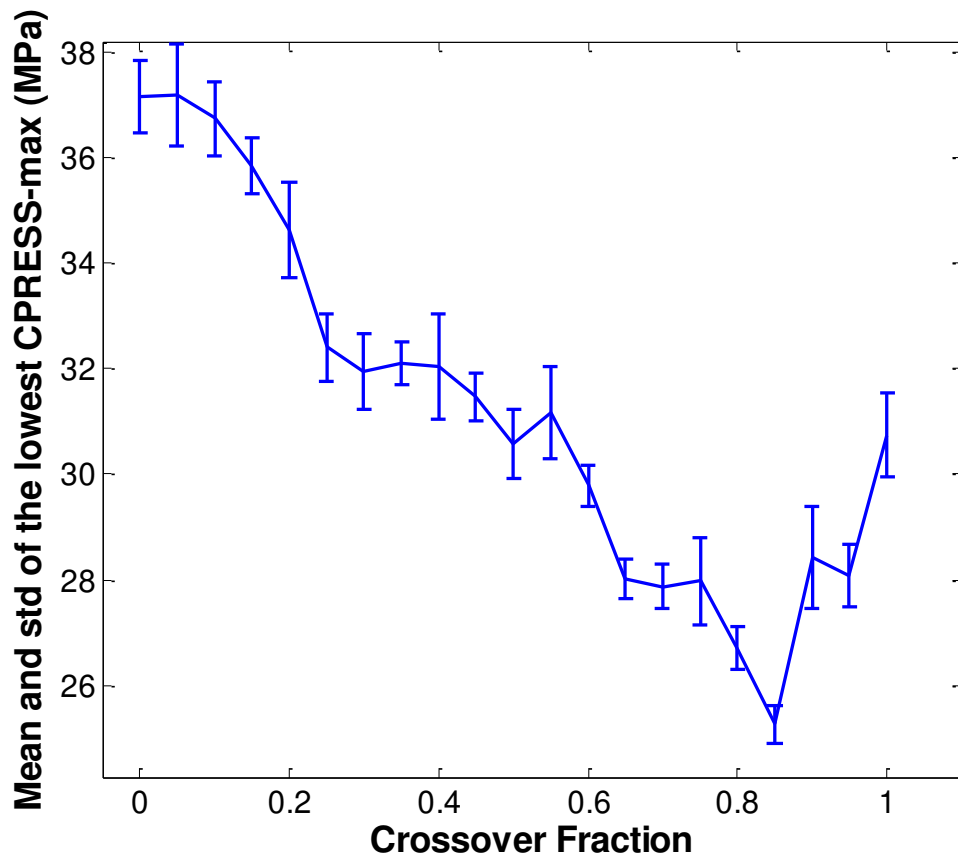
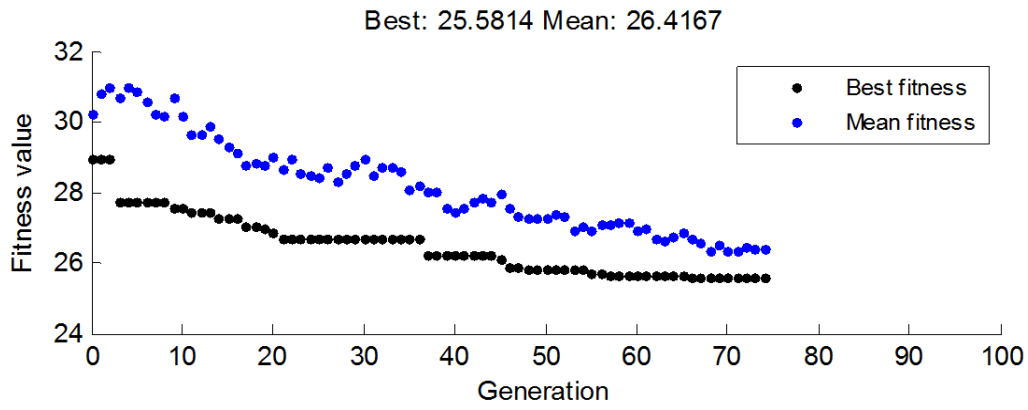
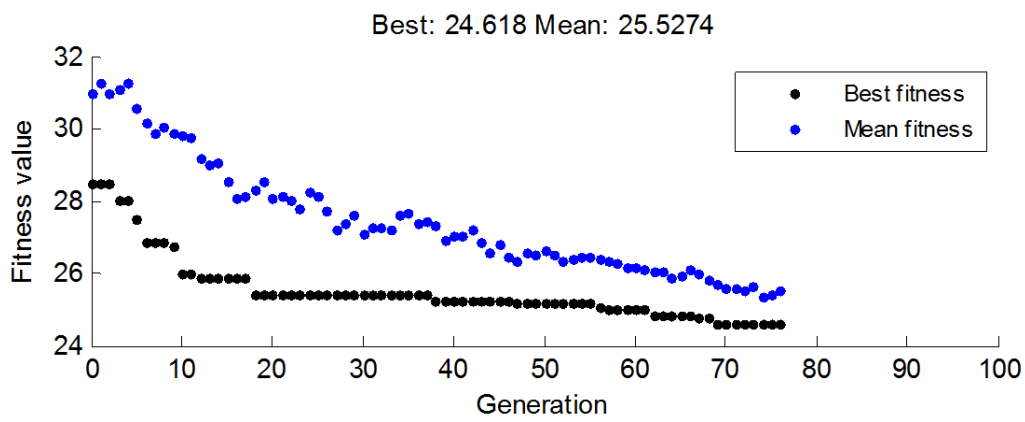


Figure 5 Mean and standard deviation of the optimized CPRESS-max for different values of crossover fraction in the GA process.

Figure 6



(a)



(b)

Figure 6 Convergence of the GA for (a) the first optimization problem in which the knee flexion angle was bounded to normal patterns,(b) the second optimization problem in which the knee flexion angle was allowed to increase beyond normal pattern. “fitness” refers to the calculated value of CPRESS-max for each individual.

Figure 7

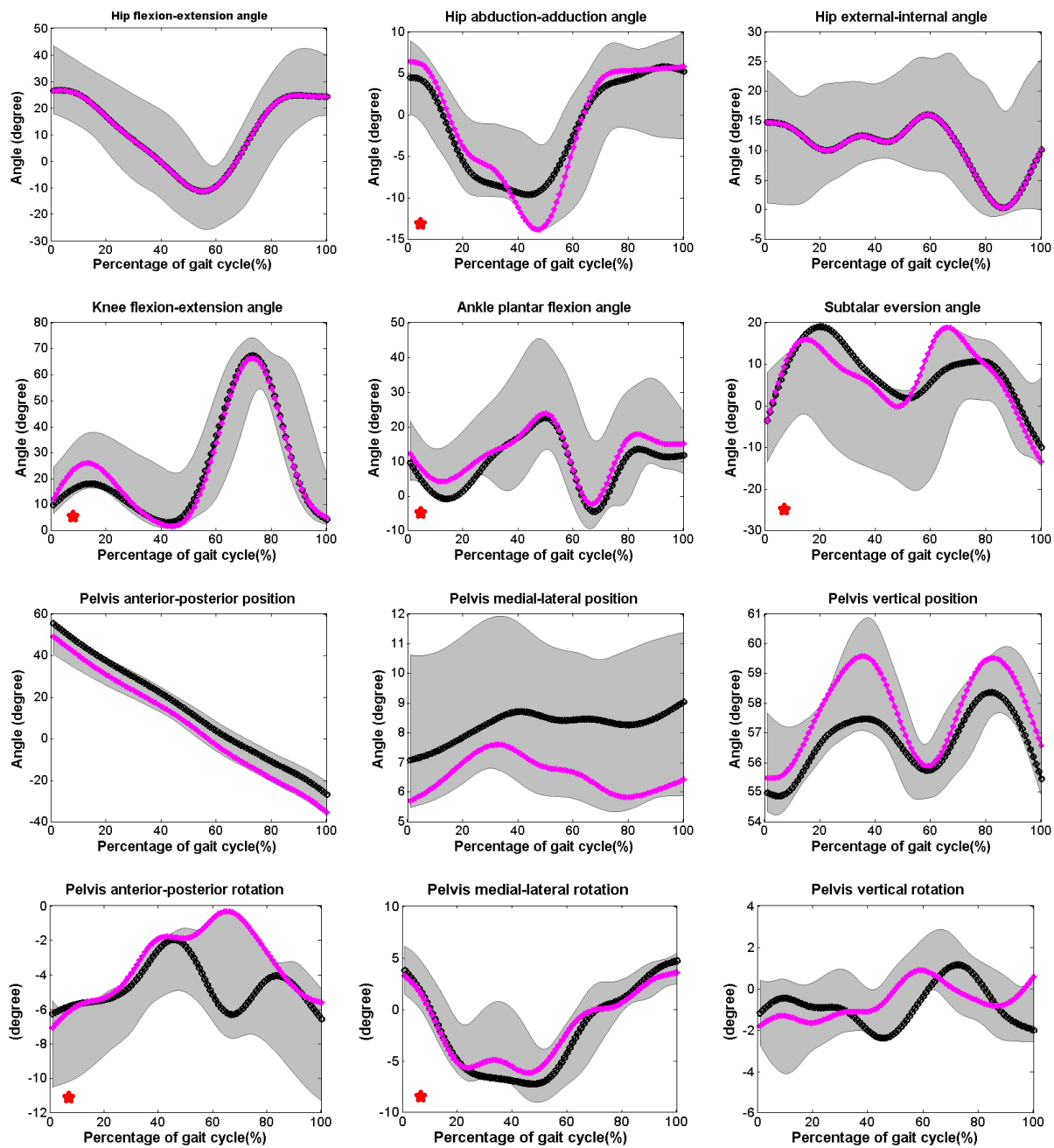


Figure 7 Kinematics of the first optimized gait pattern (black line) and the second optimized pattern (pink line) laid within the extent of experimental gait trials (gray span). Those kinematics that underwent considerable changes have been marked by *

Figure 8

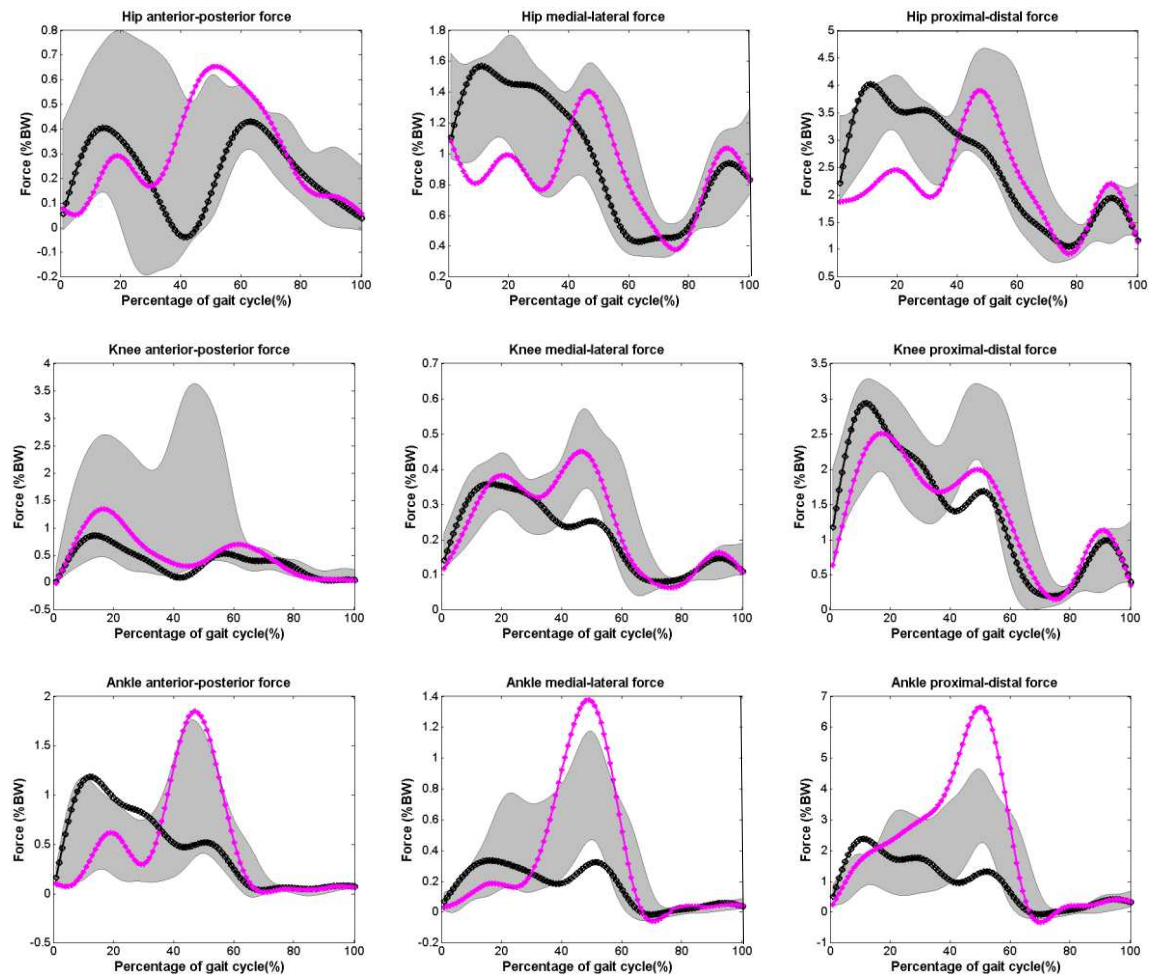


Figure 8 Resultant joint contact forces of the first optimized gait pattern (black line) and the second optimized pattern (pink line) laid within the extent of experimental gait trials (gray span).

Figure 9

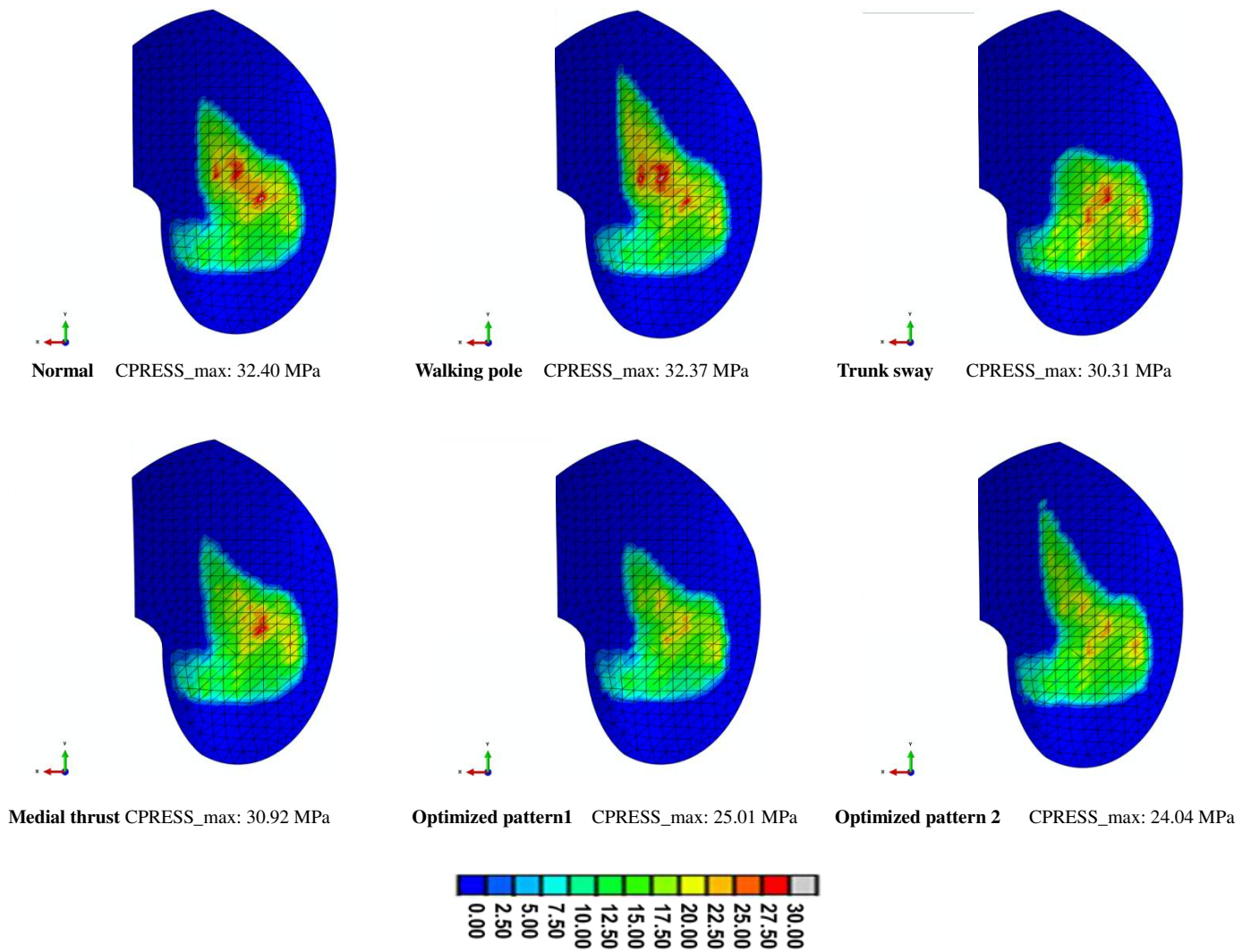


Figure 9 The resultant maximum values of contact pressures for the optimized gait patterns versus contact pressures obtained from normal gait and other previously published gait modifications.

Supplementary Material

[Click here to download Supplementary Material: Appendix.docx](#)